

## Research Article

# Simple, Compact, and Multiband Frequency Selective Surfaces Using Dissimilar Sierpinski Fractal Elements

Clarissa de Lucena Nóbrega,<sup>1,2</sup> Marcelo Ribeiro da Silva,<sup>1,2</sup>  
Paulo Henrique da Fonseca Silva,<sup>3</sup> Adaildo Gomes D'Assunção,<sup>2</sup>  
and Gláucio Lima Siqueira<sup>1</sup>

<sup>1</sup>Pontifical Catholic University of Rio de Janeiro (PUC-Rio), 22453-900 Rio de Janeiro, RJ, Brazil

<sup>2</sup>Federal University of Rio Grande do Norte (UFRN), Caixa Postal 1655, 59078-970 Natal, RN, Brazil

<sup>3</sup>Federal Institute of Education, Science and Technology of Paraíba (IFPB), 58015-430 João Pessoa, PB, Brazil

Correspondence should be addressed to Adaildo Gomes D'Assunção; [adaildo@ymail.com](mailto:adaildo@ymail.com)

Received 7 June 2015; Revised 7 October 2015; Accepted 8 October 2015

Academic Editor: N. Nasimuddin

Copyright © 2015 Clarissa de Lucena Nóbrega et al. This is an open access article distributed under the Creative Commons Attribution License, which permits unrestricted use, distribution, and reproduction in any medium, provided the original work is properly cited.

This paper presents a design methodology for frequency selective surfaces (FSSs) using metallic patches with dissimilar Sierpinski fractal elements. The transmission properties of the spatial filters are investigated for FSS structures composed of two alternately integrated dissimilar Sierpinski fractal elements, corresponding to fractal levels  $k = 1, 2$ , and  $3$ . Two FSS prototypes are fabricated and measured in the range from 2 to 12 GHz to validate the proposed fractal designs. The FSSs with dissimilar Sierpinski fractal patch elements are printed on RT/Duroid 6202 high frequency laminate. The experimental characterization of the FSS prototypes is accomplished through two different measurement setups composed of commercial horns and elliptical monopole microstrip antennas. The obtained results confirm the compactness and multiband performance of the proposed FSS geometries, caused by the integration of dissimilar fractal element. In addition, the proposed FSSs exhibited frequency tuning ability on the multiband frequency responses. Agreement between simulated and measured results is reported.

## 1. Introduction

A periodic surface is basically a set of identical elements arranged two-dimensionally composing an infinite array [1]. A periodic array composed of conductive patches or aperture elements, acting as a reflecting or transmitting surface, is called frequency selective surface (FSS). According to the application, many parameters should be considered at the design stage of a FSS. One of the main parameters that influence the FSS frequency response is the element shape, that is, its type (patch or aperture) and geometry [1, 2].

Regarding the geometry of the conducting patch element, a FSS array can present many different shapes ranging from Euclidean to fractal geometries. The use of fractal patch geometries as conducting elements on a FSS periodic design has provided superior performance, for some applications, compared to those using typical patch geometries, such as rectangular, square, circular, dipole, cross-dipole, and square

loop [1–3]. For example, geometric fractals can be used to design single-layer FSSs with high frequency compression factors, ensuring the manufacture of compact devices [4–7]. A FSS with high frequency compression factor is referred to as compact. Furthermore, the attractive features of certain self-similar fractals allow the design of selective filters with multiband behavior [6].

In order to develop high performance spatial filters, some authors have investigated different types of periodic structures, such as reconfigurable FSSs [8], periodic arrays printed on anisotropic substrates [9], and multilayer selective filters, commonly called cascaded FSSs [10, 11].

Cascading two single-band FSS screens, using conventional patches, it is possible to obtain a dual-band frequency response. In [11], an improvement in the FSS bandwidth was obtained by cascading two FSS screens using Koch fractal elements.

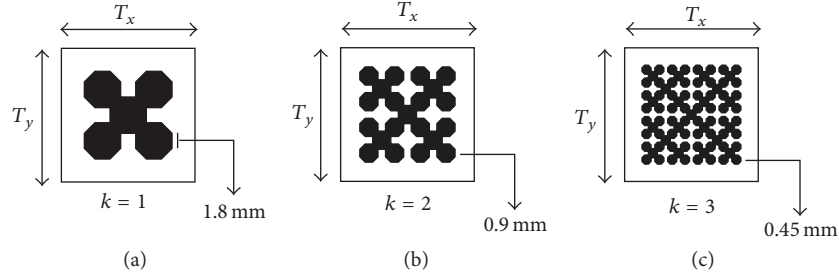


FIGURE 1: Illustration of Sierpinski patch elements of fractal levels: (a)  $k = 1$ , (b)  $k = 2$ , and (c)  $k = 3$ .

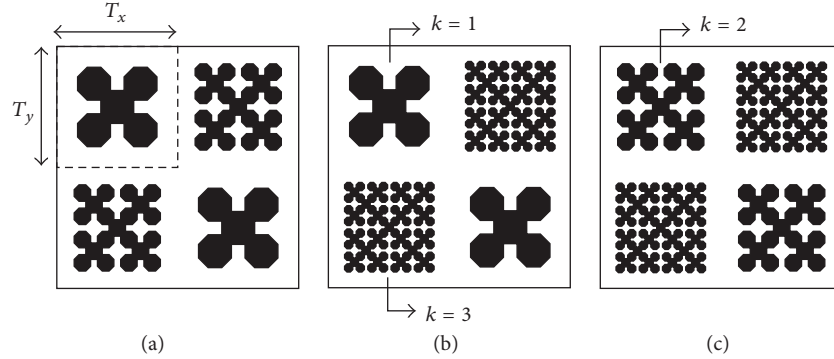


FIGURE 2: Illustrations of the proposed FSS geometries composed of dissimilar Sierpinski patch elements corresponding to the integration of (a)  $k = 1$  and  $k = 2$ , (b)  $k = 1$  and  $k = 3$ , and (c)  $k = 2$  and  $k = 3$  fractal level motifs.

In this paper we present a fractal design methodology that aims to achieve simple, compact, and multiband FSS frequency responses using dissimilar Sierpinski fractal metallic patch elements on a single-layer substrate. The Sierpinski fractal metallic patch element shapes of levels  $k = 1$ ,  $k = 2$ , and  $k = 3$  used in this work are shown in Figure 1.

The proposed FSSs with dissimilar Sierpinski metallic patches are composed of two different fractal level elements arranged alternately on the same surface, along  $x$  and  $y$  directions, as shown in Figure 2. The proposed FSS transmission properties are analyzed to design band-stop spatial filters making the adjustment of the frequency responses possible.

The FSS simulations were performed using Ansoft Designer commercial software. Two FSS prototypes were selected for fabrication and experimental characterization. The FSS prototypes were measured using a vector network analyzer from Agilent Technologies (model N5230A) and two experimental setups: (i) with elliptical monopole microstrip antennas [12] operating in the frequency range from 2 to 6 GHz (setup #1) and (ii) with horn antennas operating in the frequency range from 7 to 12 GHz (setup #2). Alternatively to the use of commercial horn antennas, we used two ultrawideband (UWB) elliptical monopoles for accurate and low-cost FSS measurements with good performance at S and C microwave bands [12].

## 2. FSS Geometries and Results

In this work new FSS geometries are proposed based on the alternately integration, along the structure horizontal,  $x$ , and

vertical,  $y$ , directions of dissimilar Sierpinski fractal patch elements, as illustrated in Figure 2. There are other possible combinations of the FSS fractal patch elements. However, we chose FSSs with two alternating fractal levels to get symmetry and the same responses for TE and TM polarizations.

The main goal of this work is to enhance the multiband response and compactness of the proposed FSS geometries with dissimilar Sierpinski fractal elements with respect to those of FSS geometries with identical Sierpinski fractal elements [7]. Figures 2(a), 2(b), and 2(c) show the proposed FSS geometries composed of dissimilar Sierpinski patch elements with (a)  $k = 1$  and  $k = 2$ , (b)  $k = 1$  and  $k = 3$ , and (c)  $k = 2$  and  $k = 3$  fractal level motifs, respectively. Simulations of these FSS geometries were performed using Ansoft Designer.

Thereafter, two FSS prototypes were fabricated for experimental characterization and comparison purpose. Figure 3 presents the photographs of the manufactured FSS structures. However, only sixteen unit cells of each FSS are shown, to improve viewing. These FSS prototypes were fabricated by printing dissimilar fractal elements alternately on single dielectric layers of RT/Duroid 6202, with relative permittivity  $\epsilon_r = 2.94$ , loss tangent  $\tan \delta = 0.0015$ , thickness  $h = 1.5$  mm, and array periodicity  $T = T_x = T_y = 16$  mm. Figure 4 shows two experimental setups used for FSS measurements: setup #1 with elliptical monopoles (Figure 4(a)) and setup #2 with horn antennas (Figure 4(b)).

The transmission coefficient simulated results for the FSSs presented in Figures 2(a), 2(b), and 2(c) are shown in Figures 5(a), 5(b), and 5(c), respectively. In addition, to point out the

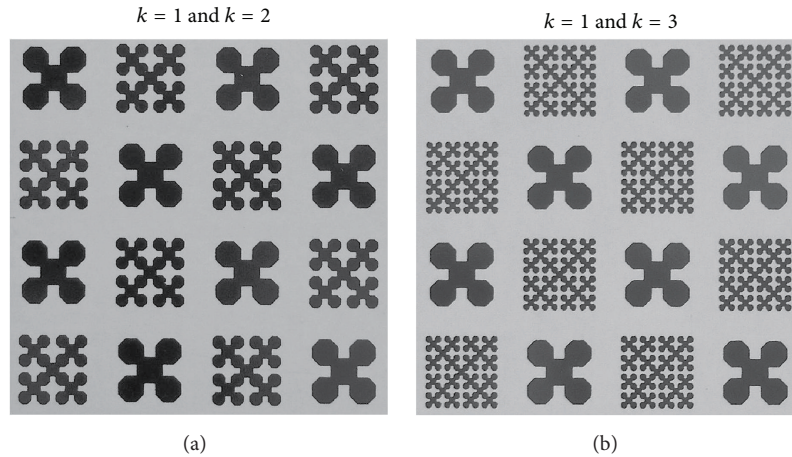


FIGURE 3: Photographs of two FSS prototypes composed of dissimilar Sierpinski patch elements with (a)  $k = 1$  and  $k = 2$  and (b)  $k = 1$  and  $k = 3$  fractal level motifs.

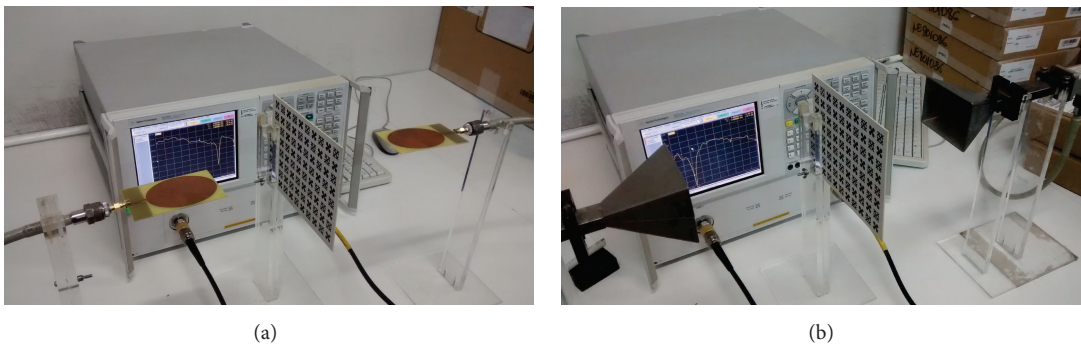


FIGURE 4: Photographs of the experimental setups: (a) setup #1 with elliptical monopoles and (b) setup #2 with horn antennas.

effect on the frequency response of the proposed FSS structures (with two dissimilar Sierpinski fractal patch elements), we included in Figures 5(a), 5(b), and 5(c) the obtained results for each one of the integrated fractal level motifs. For example, in Figure 5(a), corresponding to the FSS geometry with the integration of  $k = 1$  and  $k = 2$  fractal level elements (FSS with two dissimilar elements shown in Figure 2(a)), we included results obtained, separately, for the FSS geometries with  $k = 1$  or  $k = 2$  identical fractal level motifs.

In Figure 5(a), observe that the FSS geometry composed of dissimilar Sierpinski patch elements with  $k = 1$  and  $k = 2$  fractal levels (Figure 2(a)) enabled two resonant frequencies, indicating a dual-band operation, different from the single-band responses obtained, separately, for the FSSs with identical  $k = 1$  or  $k = 2$  fractal level motifs. Furthermore, the first and second resonant frequency values for the FSS with dissimilar elements are lower than the closest ones of the two FSSs with ( $k = 1$  or  $k = 2$ ) identical elements, confirming the patch element size reduction and tuning ability of the integrated geometry.

In Figure 5(b), observe that the FSS geometry composed of dissimilar Sierpinski patch elements with  $k = 1$  and  $k = 3$  fractal levels (Figure 2(b)) enabled three resonant frequencies, indicating a triple-band operation, different from

the single-band response obtained for the FSS with  $k = 1$  identical fractal level elements and from the dual-band response obtained for the FSS with  $k = 3$  identical fractal level elements. Similarly, the three resonant frequency values for the FSS with dissimilar elements are lower than the closest ones of the two FSSs with ( $k = 1$  or  $k = 3$ ) identical elements.

In Figure 5(c), observe that the FSS geometry composed of dissimilar Sierpinski patch elements with  $k = 2$  and  $k = 3$  fractal levels (Figure 2(c)) enabled four resonant frequencies, indicating a quad-band operation, different from the single-band response obtained for the FSS with  $k = 2$  identical fractal level elements and from the dual-band response obtained for the FSS with  $k = 3$  identical fractal level elements. Observe that three of the four resonant frequency values for the FSS with dissimilar elements correspond to reduced values of the two FSSs with ( $k = 2$  or  $k = 3$ ) identical elements. The novelty in this case is the generation of a fourth resonance frequency at about 11.4 GHz, confirming the multiband performance of the integrated FSS geometry.

Table 1 presents numerical values for the investigated FSS main parameters such as resonant frequency,  $f_r$ , and impedance bandwidth, BW, for a  $-10$  dB reference level.

Figure 6 shows a comparison between simulated and measured transmission coefficient results for the fabricated

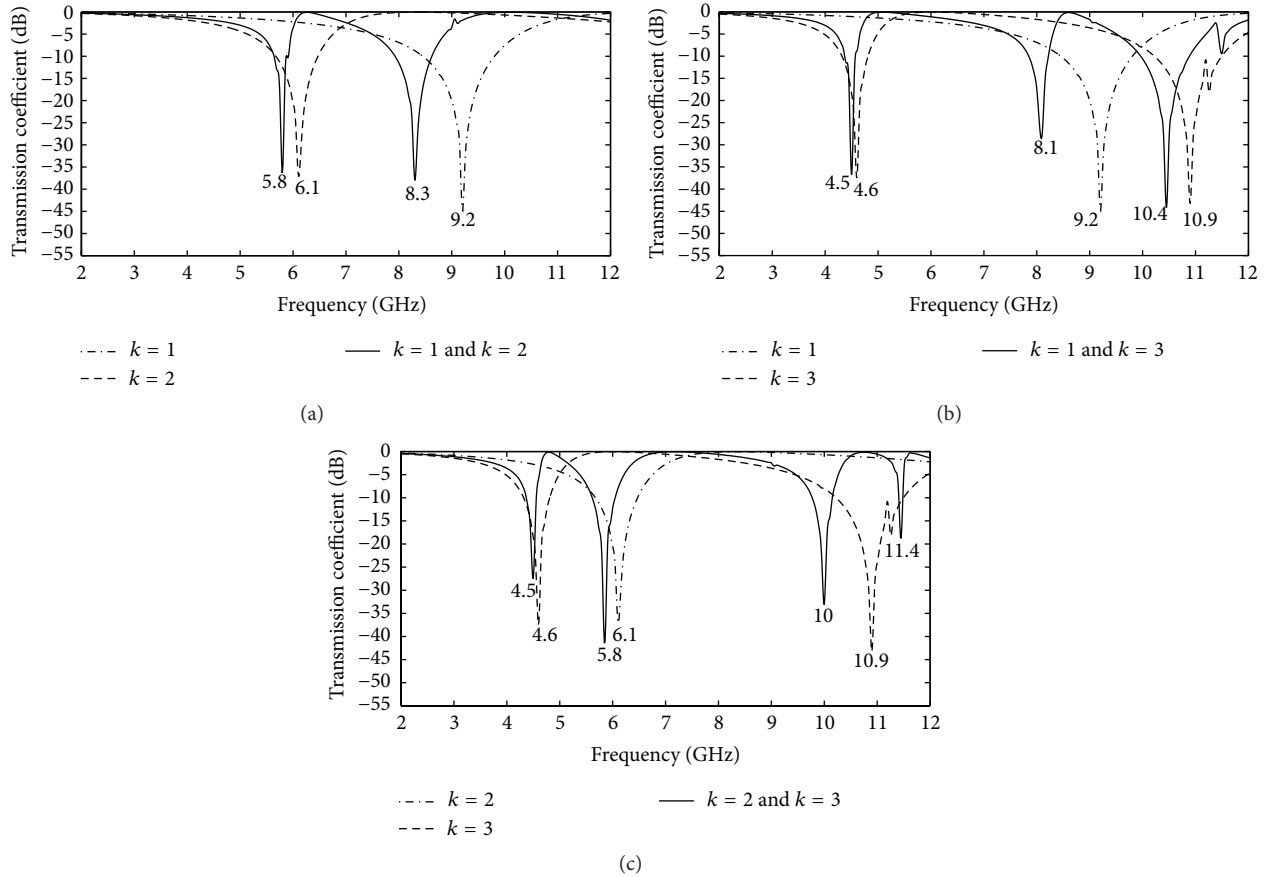


FIGURE 5: Simulated transmission coefficient results versus frequency obtained for the proposed spatial filters with two dissimilar Sierpinski fractal patch elements and for the FSS geometries with identical fractal level: (a)  $k = 1$ ,  $k = 2$ , and  $k = 1$  and  $k = 2$ , (b)  $k = 1$ ,  $k = 3$ , and  $k = 1$  and  $k = 3$ , and (c)  $k = 2$ ,  $k = 3$ , and  $k = 2$  and  $k = 3$ .

TABLE 1: Simulated FSS resonant frequencies and bandwidths.

Fractal level	FSS simulated results (GHz)							
	$f_{r1}$	BW <sub>1</sub>	$f_{r2}$	BW <sub>2</sub>	$f_{r3}$	BW <sub>3</sub>	$f_{r4}$	BW <sub>4</sub>
$k = 1$	9.2	1.36	—	—	—	—	—	—
$k = 2$	6.1	0.8	—	—	—	—	—	—
$k = 3$	4.6	0.49	10.9	1.28	—	—	—	—
$k = 1$ and $k = 2$	5.8	0.27	8.3	0.7	—	—	—	—
$k = 1$ and $k = 3$	4.5	0.2	8.1	0.37	10.4	0.92	—	—
$k = 2$ and $k = 3$	4.5	0.19	5.8	0.43	10	0.38	11.4	0.08

FSS prototypes. Figure 6(a) presents the results for the FSS spatial filter with Sierpinski fractal elements of levels  $k = 1$  and  $k = 2$ . Figure 6(b) presents the results for the FSS prototype with Sierpinski fractal patches of levels  $k = 1$  and  $k = 3$ .

The experimental characterization of the proposed FSSs was performed using a vector network analyzer, two UWB elliptical monopole microstrip antennas, for the frequency range from 2 to 6 GHz (setup #1), and two commercial horn

antennas, for the frequency range from 7 to 12 GHz (setup #2). Measured and simulated results are in good agreement, with a maximum resonant frequency deviation of 4.8%. Simulations were performed using Ansoft Designer.

### 3. Conclusions

In this work, simple, compact, and multiband frequency selective surface (FSS) structures were obtained by integrating dissimilar Sierpinski fractal patch elements. The proposed FSS geometries enabled the development of multiband band-stop filters due to the integration of dissimilar fractal patch elements on a single-layer substrate and the FSS element size reduction, provided by the fractal motifs. In addition, the use of dissimilar Sierpinski fractal geometries to design FSS elements also provided resonant frequency and bandwidth adjustments. Furthermore, the FSS design methodology, using alternately dissimilar fractal elements, was validated by means of a good agreement between simulated and measured results. The proposed FSS geometries may be used in many engineering applications, being attractive devices due to low cost, easy manufacturing, and ease integration with other

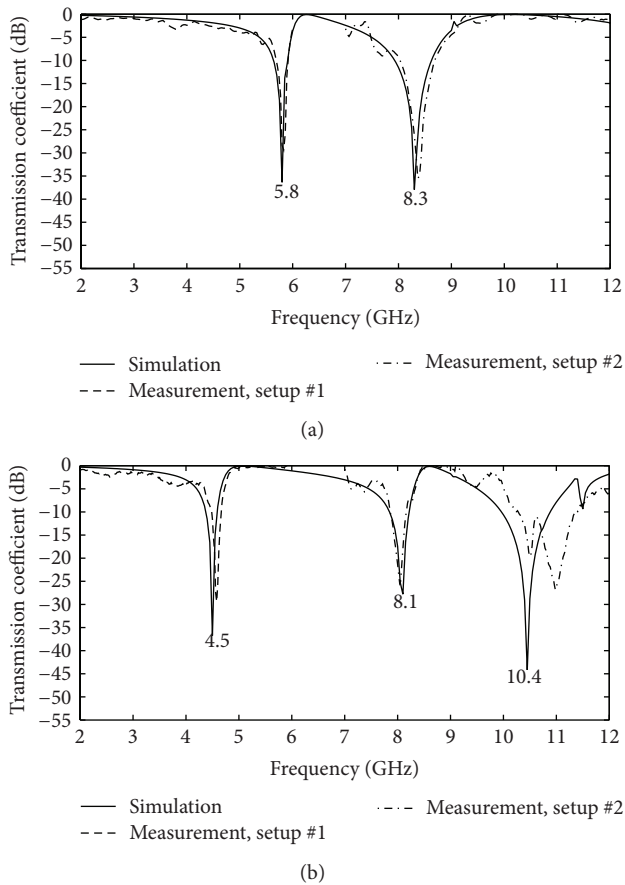


FIGURE 6: Simulated and measured transmission coefficient results versus frequency for the fabricated FSS prototypes integrating dissimilar Sierpinski fractal patch elements of levels: (a)  $k = 1$  and  $k = 2$  and (b)  $k = 1$  and  $k = 3$ .

microwave circuits. Currently, multiband FSSs have been proposed to be applied in modern civil construction designs to optimize indoor propagation environments.

### Conflict of Interests

The authors declare that there is no conflict of interests regarding the publication of this paper.

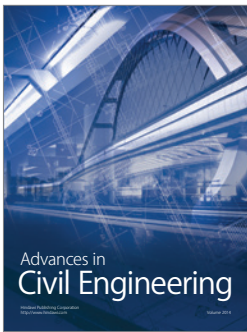
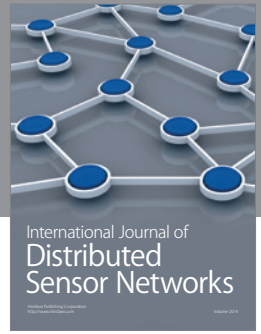
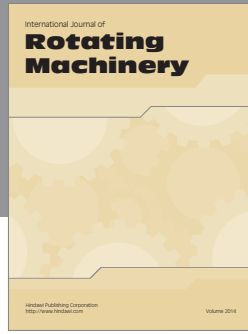
### Acknowledgments

This work was supported by CNPq under covenant 573939/2008-0 (INCT-CSF) and contract 307554/2012-0, Federal Institute of Education, Science and Technology of Paraíba (IFPB), and Federal University of Rio Grande do Norte (UFRN).

### References

- [1] T. K. Wu, *Frequency Selective Surface and Grid Array*, John Wiley & Sons, New York, NY, USA, 1995.
- [2] B. A. Munk, *Frequency Selective Surfaces: Theory and Design*, John Wiley & Sons, New York, NY, USA, 2005.

- [3] W. Li, C. Wang, Y. Zhang, and Y. Li, "A miniaturized frequency selective surface based on square loop aperture element," *International Journal of Antennas and Propagation*, vol. 2014, Article ID 701279, 6 pages, 2014.
- [4] W. T. Wang, P. F. Zhang, S. X. Gong, B. Lu, J. Ling, and T. T. Wan, "Compact angularly stable frequency selective surface using hexagonal fractal configurations," *Microwave and Optical Technology Letters*, vol. 51, no. 11, pp. 2541–2544, 2009.
- [5] R. Natarajan, M. Kanagasabai, S. Baisakhiya, R. Sivasamy, S. Palaniswamy, and J. K. Pakkathillam, "A compact frequency selective surface with stable response for WLAN applications," *IEEE Antennas and Wireless Propagation Letters*, vol. 12, pp. 718–720, 2013.
- [6] M. R. Silva, C. L. Nóbrega, P. H. F. Silva, and A. G. D'Assunção, "Stable and compact multiband frequency selective surfaces with peano pre-fractal configurations," *IET Microwaves, Antennas & Propagation*, vol. 7, no. 7, pp. 543–551, 2013.
- [7] C. L. Nóbrega, M. R. Silva, P. H. F. Silva, and A. G. D'Assunção, "A compact frequency selective surface with angular stability based on the Sierpinski fractal geometry," *Journal of Electromagnetic Waves and Applications*, vol. 27, no. 18, pp. 2308–2316, 2013.
- [8] J. M. Zendejas, J. P. Gianvittorio, Y. Rahmat-Samii, and J. W. Judy, "Magnetic MEMS reconfigurable frequency-selective surfaces," *Journal of Microelectromechanical Systems*, vol. 15, no. 3, pp. 613–623, 2006.
- [9] D. X. Wang, E. K. N. Yung, and R. S. Chen, "Spectral domain analysis of frequency-selective surfaces on biaxially anisotropic substrate," *IET Microwaves, Antennas & Propagation*, vol. 1, no. 2, pp. 335–340, 2007.
- [10] L. Moustafa and B. Jecko, "Bandwidth improvement of EBG resonator antennas using double-layer FSS," *International Journal of Antennas and Propagation*, vol. 2008, Article ID 315052, 5 pages, 2008.
- [11] A. L. P. S. Campos, R. H. C. Maniçoba, and A. G. D'Assunção, "Investigation of enhancement band using double screen frequency selective surfaces with koch fractal geometry at millimeter wave range," *Journal of Infrared, Millimeter, and Terahertz Waves*, vol. 31, no. 12, pp. 1503–1511, 2010.
- [12] C. L. Nóbrega, M. R. Silva, P. H. F. Silva, and A. G. D'Assunção, "Experimental characterization of FSS for WLAN applications with low-cost UWB elliptical microstrip monopole antennas," *Microwave and Optical Technology Letters*, vol. 56, no. 6, pp. 1331–1333, 2014.



**Hindawi**

Submit your manuscripts at  
<http://www.hindawi.com>

